Long-Term Cognitive Deficits After Traumatic Brain Injury Associated With Microglia Activation

Esber Saba
American University of Beirut
Mona Karout
American University of Beirut
Leila Nasralla
American University of Beirut
Firas Kobeissy
American University of Beirut
Hala Darwish
American University of Beirut
Samia Khoury (sk88@aub.edu.lb)
American University of Beirut

Research Article

Keywords: Traumatic brain injury, Microglia, Cognition, Spatial Memory, Infiltrating Macrophages, Chronic Inflammation

Posted Date: June 30th, 2021

DOI: https://doi.org/10.21203/rs.3.rs-429333/v2

Version of Record: A version of this preprint was published at Clinical Immunology on September 1st, 2021. See the published version at https://doi.org/10.1016/j.clim.2021.108815.

Abstract

Traumatic Brain Injury (TBI) is the most prevalent of all head injuries, and based on the severity of the injury, it may result in chronic neurologic and cognitive deficits. Microglia play an essential role in homeostasis and diseases of the central nervous system. We hypothesize that microglia may play a beneficial or detrimental role in TBI depending on their state of activation and duration.

In the present study, we evaluated whether TBI results in a spatiotemporal change in microglia phenotype and whether it affects sensory-motor or learning and memory functions in male C57BL/6 mice. We used a panel of neurological and behavioral tests and a multi-color flow cytometry-based data analysis followed by unsupervised clustering to evaluate isolated microglia from injured brain tissue. We characterized several microglial phenotypes and their association with cognitive deficits. TBI results in a spatiotemporal increase in highly activated microglia that correlated negatively with spatial learning and memory at 35 days post-injury. These observations could define therapeutic windows and accelerate translational research to improve patient outcomes.

Introduction

Microglia are the central nervous system (CNS) resident innate immune cells that play critical physiological roles in the healthy and injured brain. They detect and rapidly respond to any disruption in the status quo of the CNS, including infections or tissue injury, and often act to remove cellular debris [1]. The activation of microglia from their resting surveillance state occurs within minutes of the injury and is critical for recovery. However, prolonged activation may be detrimental and contribute to secondary damage. When the microglia are activated in response to any disruption, this activation alters their gene expression and morphology [2]. Although they have distinctive lineage, microglia resemble blood-derived macrophages that infiltrate the CNS from the periphery in response to tissue damage [3]. Microglia are usually classified into the classical M1 phenotype that is considered proinflammatory, and the M2 anti-inflammatory is thought to be involved in neural repair [4]. However, more recent data suggest that microglia's activation status is on a continuum between anti- and pro-inflammation rather than a rigid dichotomous phenotype [5].

Chronic neuroinflammatory response to an acquired brain insult such as a TBI contributes to the injury and lengthens or halts recovery [6]. In chronic neuroinflammation, microglia remain activated for an extended period during which the production of repair mediators is sustained longer than usual [7]. Of note, chronic microglial activation has also been linked to most, if not all, neurodegenerative diseases like Alzheimer’s disease, amyotrophic lateral sclerosis, and Parkinson’s disease [8–10]. In humans with traumatic brain injury (TBI), microglial activation has been reported as early as 72 hours after injury [11], and it can persist for months after injury [12].

TBI is the most prevalent of all CNS injuries and results in chronic neurologic and cognitive deficits [13]. TBI causes cell death and neurologic dysfunction through secondary injury mechanisms characterized by

edema, neuronal cell death, glial activation, and infiltration of peripheral immune cells [14]. Extensive research has been conducted investigating the role of microglia after head injury and its interaction with the neural microenvironment suggesting a role for microglia in the injury process as well as in neurotransmission and maintenance of synaptic integrity [15]. TBI initiates a neuroinflammatory cascade that persists over time and may lead to prolonged cognitive deficits. The regional distribution of microglial activation is yet to be determined. Some studies found chronic activation in the thalamus, others in the hippocampus in addition to the injury site [16]. Despite evidence showing a significant role for microglia in the pathogenesis of TBI, no studies to date have examined the spatiotemporal microglial activation response after injury and explored its potential correlation with cognitive deficits [17–19].

Here we hypothesized that TBI would result in phenotypic changes in the microglial cell population that persists for a long time after the injury. We also hypothesized that chronic microglial activation is associated with cognitive deficits. We analyzed the spatiotemporal course of microglia changes isolated from the injured brain up to 35 days after controlled cortical impact (CCI) in mice. We used conventional flow cytometry techniques followed by bioinformatics-based multi-parametric methods that are not constrained by assumptions or bias. We observed heterogeneity in microglia phenotypes and temporal changes in microglia subpopulations following TBI. A particular subpopulation that we called hyperactivated microglia was correlated with chronic deficits in learning and spatial memory after injury.

Methods

Animals

The Institutional Animal Care and Utilization Committee (IACUC) of the American University of Beirut (AUB) approved this study. The study is reported in accordance with ARRIVE guidelines[64]. C57BL/6 mice were obtained from the Animal Care Facility of the American University of Beirut and housed in a controlled environment (12 h reverse light/dark cycles, 22 ± 2°C). All efforts were made to reduce the number of animals used and their suffering. All animals were handled and fed regular chow and water ad libitum.

Controlled cortical impact injury (CCI) model.

Open head injury was performed to induce TBI in mice, using the electromagnetic controlled cortical impact device (Leica Impact One Angle with Leica Angle Two™ Stereotaxic Instrument, Biosystems, Buffalo Grove, IL, USA), as described previously [65]. Briefly, adult (8 weeks old) C57BL/6 mice (~ 22–25 g, n = 30) were anesthetized with a mixture of Ketamine (50 mg/kg, Panpharma) and Xylazine (15 mg/kg, Interchemie), injected intra-peritoneally. Animals were placed in a stereotactic frame in a prone position and secured by ear and incisor bars. The target site was set parasagittal between Bregma and Lambda (somatosensory area of the parietal cortex) with standard coordinates (+ 1.0 mm AP, + 1.5 mm ML, and − 2 mm DV), where craniotomy was made. Bone was removed using a drill, and the injury was induced by impacting the left cortex with a pneumatic piston containing a 1 mm diameter tip at a rate of 4 m/s. Mild

CCI in the somatosensory area was produced with an impact of 0.5 mm depth, whereas severe CCI with 2 mm depth into the cortical tissue. The animals were rapidly removed from the stereotaxic frame, sutured, and kept in a holding cage on a heating pad until recovery from anesthesia. In sham-operated control mice, anesthesia was given, and a craniotomy was performed, but no injury was induced. To estimate the lesion volume, a series of the five brain sections of each animal were stained with hematoxylin and eosin (H & E staining) and analyzed using a 1.6 × objective and a computer image analysis system ImageJ. Each hemisphere's volume was calculated by measuring the hemisphere's area, subtracting the lesion area from each section, and multiplying by the section thickness and the sampling interval based on Paxinos and Watson atlas of the mouse brain (Fig. 9).

Neurological tests

A total of 30 mice were used, randomized into 3 groups: sham, mild TBI (mTBI), and severe TBI (sTBI), of 10 mice each. Mice (~ 20 g, 6 weeks old) were allowed two weeks of habituation after arrival and handled for 7 consecutive days before surgery. After the injury (D0), the neurological and cognitive tests were performed, using: Pole climbing, adhesive removal test, spontaneous object and location recognition memory tests, and the Morris water maze, at three different time-points: acute 48 hours, subacute 7 days, and chronic 35 days. Animals were sacrificed and used for microglia isolation.

Pole climbing test

This test assesses motor performance and coordination in mice [66]. Each mouse was placed head up on the top of a vertical rod (height = 60 cm, diameter = 1 cm). The mouse is supposed to turn and descend by gripping without slipping. The time needed for the mouse to reach the bottom (t-total) was recorded; also, the t-turn (time at which the mouse turned head down on the rod), the t-half (time at which the mouse reached half of the rod), and the t-stop (Amount of time the mouse stopped on the rod), were recorded.

Adhesive removal test

The adhesive removal test, a sensory measure, was performed 48h, 7 days, and 35 days post-TBI. Three consecutive experimental trials were conducted for each mouse. Briefly, a strip of tape (0.5 cm x 0.5cm dimensions) was placed on the mouse snout, and the time needed for each mouse to sense (Time-to-contact) and remove (Time-to-remove) the adhesive tape was recorded.

Spontaneous object and location recognition memory (OR)

Spontaneous object recognition depends on the innate capacity of rodents to discriminate a novel from a familiar object (previously encountered). The test was performed as described previously [67]. Briefly, mice were placed in the center of an open field at the beginning of each trial and freely explored the open field and objects. At the end of each trial (5min), mice were removed from the open fields and placed in their home cages next to each testing area for the inter-trial interval (ITI-5 min). The open fields and objects were cleaned with 70% ethanol during the ITI. During Trial 1, the animal explored an empty open field. During trials 2 to 4, three identical objects were placed near the corners of each open field. The objects'

configuration remained unchanged during trials 2 to 4 to allow the mice to encode the objects' shape and location. Object recognition was examined in Trial 5 and 6 after replacing one familiar object with a novel object. Object recollection or response to spatial novelty was examined in Trial 7–8 after moving the novel object to a new location in the open field. All data were recorded by a video camera suspended above the 4 open fields and connected to image analyzer software (Any Maze-IL-USA®). The zones were located 5 cm around each object on the software, and the software recorded the time the animal spent in each zone with their head directed toward the object.

Morris Water Maze (MWM)

To test spatial learning and memory, the Morris Water Maze was used. The animals learn the location of a submerged platform using constellations of external cues. The MWM was conducted as previously described [68]. A fixed submerged platform was placed within the pool for the animals to use as an escape. On Day 31 post-trauma, all the animals were placed in a circular dark-colored water tank, 0.55-meter depth and 1-meter diameter, filled with room temperature water (25–26°C) made opaque by adding Tempera® washable, non-toxic white paint. An invisible transparent escape platform of 30 cm height and 10 cm diameter was placed in the mid-NE quadrant, 1.5 cm below the water's surface. The pool was in a large testing room, where there were at least 3 external and visible cues such as pictures. The cues and the experimenter's location (North-East quadrant) were kept constant throughout the experiment. Each mouse was tested for 4 consecutive days, 3 trials per day, and on day 35, only 1 probe trial was performed; the platform is removed from the pool, and the time the animals spend searching where the platform was located is measured. Typically, the normal animal will spend more time searching in the quadrant where the platform was located, indicating spatial memory. The pool was divided into four equal quadrants designated as North East, South East, North West, and South West. At the start of each trial, each mouse was placed in one of the four quadrants. The starting point was fixed in the South quadrant, followed by North, then East, and West. Only on the first testing day, a one-minute trial 0 was performed before the learning trials. Trial 0 was conducted with a visible flag attached to the visible platform to guide the animal to the platform and ensure the animals do not have any visual deficits. Following trial 0, the platform was submerged, and the animals were expected to locate the platform based on their spatial learning and memory. The mice were then placed in each quadrant facing the tank's wall and allowed to swim until they found the platform or for a maximum of 60 seconds. Once the animals reached the platform, they were left on it for 30 seconds before being returned to their cage for an inter-trial interval of 60 seconds. If the animal was unable to find the platform within 60 seconds, the trial was terminated. In this case, the experimenter guided the animal to the platform and allowed it 30 seconds of exploration before returning to its' cage. Time spent to find the platform (latency to escape-NE) during the testing days was used to evaluate spatial learning. Time to reach the platform or escape latency is commonly used to assess spatial learning; here, we slightly changed the presentation of the results by calculating cumulative (total of 3 trials/day) latency to the platform that accounts for acquisition and incremental spatial learning of all trials. On day 35 (probe trial), the percentage time traveled in the target zone was used as an index of spatial memory. A video camera recorded the

performance, and the time spent in each quadrant was acquired and analyzed using an automated tracking system (Any Maze-IL-USA®).

Microglia isolation and Flow Cytometry

After completing the neurological and learning and memory tests, the mice were sacrificed at acute (48hrs), sub-acute (7-days), and chronic (35-days) time points. Brains were collected and dissected to isolate the different regions of interest: the hippocampus, the thalamus, and the cortex from the contralateral and the ipsilateral hemispheres [69]. Briefly, after brain dissociation, immune cells were enriched over a percoll gradient to remove myelin and other debris, protocol adapted from [70]. The cells were then labeled with antibodies against CD11b, CD45, F4/80, CX3CR1, CD68, CD206, IA/AE, and TNF-α, then measured by fluorescence-activated cell sorting (FACS) (Table 1).

Table 1
Fluorochrome-conjugated antibodies clones.

Fluorochrome-conjugated antibody	Clone
PerCP-Cy5.5 anti- mouse CD45	30-F11
BV421/50 anti- mouse CD11b	M1/70
APC anti-mouse F4/80	BM8
PE-Cy7 anti-mouse CD206	C068C2
PE anti- mouse CD68	FA-11
FITC anti-mouse CX3CR1	SA011F11
BV610/20 anti-mouse TNFa	MP6-XT22
BV710/50 anti-mouse IA/IE	M5/114.15.2

Flow Cytometry Standard file was combined into a single flow cytometry standard file to define spatially distinct populations. Mean fluorescence intensity (MFI) is presented on a “logical” scale, as previously described [71], and viable cells were selected from all events. We next applied t-distributed stochastic neighbor embedding (TSNE), a nonlinear dimension reduction method that projects data into a lower-dimensional space. The algorithm represents the distance between any two points by the probability of these two points being neighbors [72]. We used the R package R-tsne, default parameters for TSNE implementation (iterations = 1000, perplexity = 30, θ = 0.5). Because we are interested in changes in cell populations' density across different conditions, the TSNE was followed by the unsupervised K-means clustering to cluster cells based on different markers' expression. K-means is a commonly used clustering algorithm for single-cell analysis after dimensionality reduction [73].

Statistical analysis

Unless otherwise indicated, all values presented are mean ± SEM. Fisher exact test was used to calculate the significance of categorical variables. A paired wise $\chi 2$ test with Bonferroni correction is used to compare the different clusters of cells per group and conditions after K-means clustering. We have used the Kruskal-Wallis test followed by Dunnett's post-test or ANOVA followed with Bonferroni corrections for multiple comparisons. We have used linear regression to measure the association between microglia frequencies and latency to the platform on the MWM. The two-tailed p-value was considered significant when < 0.05. The bioinformatics analysis was done using the SPSS ver.19 and Graph-pad prism 5.

Results

Neurological and cognitive assessment

Traumatic brain injury affects motor and sensory performance.

We evaluated the performance of mice on the pole climbing test. At 48h, mice with mild and severe TBI performed significantly worse than sham-injured mice as indicated by the total time taken by the animals to descend the pole (mild:11.7 ± 0.6 and severe: 21.4 ± 3.6 vs. 6.4 ± 0.8 seconds, P < 0.001 and P < 0.0001 respectively). Less time is indicative of better motor coordination and balance. Both TBI groups showed recovered motor performance at 7- and 35-days post-injury (dpi) in comparison to their performance at 48h after injury (7d: 7.1 ± 0.4 and 8.7 ± 1, P < 0.05 and P < 0.01 respectively; 35d: 8.9 ± 2 and 8.1 ± 1, P < 0.01) (Figure 1, a-d).

Furthermore, we found group differences among the sham, mTBI, and sTBI groups in time to sense and remove the stimuli on the adhesive removal test (Figure 1, e-f). At 48h post-TBI, the mean time to sense and remove the tape was significantly higher in mild and severe-TBI mice than the sham group (mild:21.4 ± 3 and severe: 25.9 ± 4 vs. sham: 8.4 ± 1.5 seconds, P < 0.05 and P < 0.01 respectively). The sensory deficit persisted on day 7 in both injury groups (mild:17.7 ± 5.8, and severe: 20.9 ± 3.5 vs. sham: 8.2 ± 3.7 seconds, P < 0.01). However, 35 days post-TBI, only the group that received severe injury showed persistent sensory deficits compared to sham (15.4 ± 2.5 vs. 7.9 ± 3.5 seconds, P < 0.05).

Severe traumatic brain injury causes long-term cognitive deficits.

Spontaneous object recognition test

During the sample phase (learning trial), the time spent acquiring information about the objects, such as size and shape, was measured as exploration time. To exclude position preference, the mean time spent exploring each object in the 3 corners of the box within each group was compared (phase 1), and no significant differences were found (data not shown). When comparing the time spent exploring the different objects during this phase, the sham group spent more time exploring all the objects at 48 h compared to animals with mild and severe TBI: (sham total exploratory time 24.9 ± 3.8 vs. mild 7.4 ± 2.7 and severe 12.9 ± 2.5 seconds, P < 0.0001 and P < 0.01 respectively).

On the Novelty test (phase 2), one familiar object was replaced with a novel one. The exploration time of the remaining two familiar objects and the novel one was compared. At all time-points, the sham animals spent more time exploring the novel object than animals with mild and severe TBI (Figure 2, a, c and e).

The same novel object was then moved to a novel position on the novel location test (phase 3). At all time-points, the sham animals spent more time exploring the novel object/location than the animals with mild and severe TBI (Figure 2, b, d, and f). Animals with mild and severe TBI, at 7- and 35-days post-trauma, showed persistent impaired spontaneous object recognition compared to the sham animals.

The Morris water maze test

Both the sham and mTBI mice showed similar learning curves 31-35 days post-injury. However, as expected, a longer latency to the platform was found after a severe TBI compared to the Sham and mTBI on all days. The group with severe TBI showed little learning during the four trial days, indicating impaired spatial learning that persisted up to 35 days (Figure 3, a). When examining the percentage time spent in the target quadrant and the latency to correct quadrant (data not shown), the animals with mild injury were similar to the sham group, unlike the animals post severe TBI who remained significantly impaired. The same was found when we examined the percentage of time spent swimming in the correct quadrant on the probe trial (Figure 3, b) (day 5). The animals with mTBI performed like the sham and remembered where the platform was located, whereas the animals with a severe injury did not, indicating impaired spatial memory (Figure 3, c).

Microglia Isolation and typing

Conventional Flow cytometry analysis identified microglia and infiltrating macrophages.

To investigate the dynamics of microglial activation following TBI, we isolated microglia from different brain regions: hippocampus, thalamus, and cortex ipsilateral and contralateral to the injury site. Live cells were stained with anti-CD11b, CD45 and CX3CR1. Figure 4 a-b shows representative flow cytometry scatter plots that were used to measure the frequency of microglia in the different parts of the brain. Interestingly, starting at 48 hours post-TBI the frequency of isolated microglia ($CX3CR1^{hi}$) increased in all regions studied in both mild and severe TBI groups. In the mild TBI group the increase in microglia was significant in the ipsilateral cortex at 48 hours, and in both ipsi- and contralateral cortices at 7 days. While in the severe TBI group, a significant increase was noted in all investigated regions at 48 hours. This increase in frequency remained significant in the cortical areas and hippocampi on days 7 and 35 (except for the ipsilateral cortex on day 35). The thalamus showed significantly increased microglia frequency at 48 hours bilaterally, but only the increase in the ipsilateral thalamus remained significant at day 7 and the contralateral thalamus on day 35. Furthermore, myeloid cells ($CD45^{hi}$ $CX3CR1^{lo}$) likely representing infiltrating macrophages were detected at 48h in the ipsilateral side in the three investigated brain regions of the severe TBI group only. These cells were not detected at subacute and chronic time points. The increase of microglia numbers in both hemisphere of injured mice reflects a diffuse injury that extends beyond the injury site.

Microglia activation markers, mainly CD11b, CD206, TNFa and AIEI, were found upregulated at 48h post-injury. Even though the markers were increased in both hemispheres, the highest MFIs were noted on the ipsilateral side. As one would expect, microglia markers followed the same dynamics as observed for the cell frequencies in figure 4 c. almost all activation markers that were upregulated at the early time point return to baseline on day 7. However, on day 35 we observed a re-emergence of these markers in the brains of the severe TBI group. The increase of IAIE, which is considered a marker of activation in microglia [20], at this later time point suggests that microglia are chronically activated. The activation was noticeable at the level of the ipsilateral Hippocampus and the contralateral thalamus and cortex (figure 5). TNFa, the inflammatory cytokine, was found to follow the same pattern as Class II, suggesting that the chronically activated microglia are likely proinflammatory (Data not shown).

Non-linear Dimensionality Reduction Reveals Multiple Distinct Microglia Cell States

To investigate the phenotypic heterogeneity and dynamics of cells after traumatic brain injury, we used the combination of 8 markers projected into the two-dimensional space followed by cluster analysis. This method allowed the characterization of several subpopulations of cells.

The markers CD11b and TNFa contributed the most to the model as was shown by the sum of square error (Figure 6, a). We identified a population of infiltrating macrophages ($CD45^{hi}$, $CD11b^{hi}$, $CX3CR1^{lo}$, CD68-, F4/80-, $CD206^{hi}$, TNFa-, IA/IE^{hi}) and three populations of microglia that were characterized by a relatively high expression of CX3CR1 and CD68. These cells could be divided into three clusters: microglia cluster 1 (CD45+, $CD11b^{hi}$, CX3CR1++, CD68++, $F4/80^{lo}$, CD206+, TNFa-, IA/IE+) microglia cluster 2 (CD45+, $CD11b^{lo}$, CX3CR1++, CD68++, $F4/80^{lo}$, CD206+, TNFa+, IA/IE+), and highly activated microglia (CD45++, $CD11b^{hi}$, $CX3CR1^{hi}$, $CD68^{hi}$, F4/80+, $CD206^{hi}$, TNFa++, IA/IE ++) (Figure 6, b).

Clusters 1 and 2 are similar for most markers, except for significantly higher CD11b and lower TNFa expression in cluster 1 compared to cluster 2. The third cluster, representing highly activated microglia, is characterized by increased expression of almost all the markers, especially TNFa and IAIE (Figure 6, c).

In the non-injured brains, the relative proportions of identified clusters were different between brain regions. The predominant population is from cluster 1, with a smaller percentage of cluster 2 cells. Interestingly, highly activated microglia are also found at a very low frequency throughout the different parts of the control brains (Figure 7). At 48 hours after TBI, we observed an increase in highly activated microglia (cluster 3) in the cortex of mild TBI animals and all brain regions of severe TBI animals. These cells resolved by day 7 in both TBI groups. Interestingly, cluster 3 cells reappeared on day 35 in the cortex and subcortical area of severe TBI mice. Furthermore, we have documented a switch in abundance between cluster 1 and cluster 2 at the injury site 48 hours dpi (Figure 7). Although cluster 2 decreases at the later time points in animals with severe TBI, these cells persist with a frequency significantly higher than in the sham group. Also, we noted an equivalent increase of cluster 2 in both the mild TBI and severe TBI 7 days post injury. However, the level of cluster 2 goes down in the mTBI group at 35 days but remains significantly higher in the severe TBI group compared to the rest of the groups. The increase in

cluster 2 types of microglia and highly activated microglia at the acute time point suggests a proinflammatory environment early after the injury in both mild and severe TBI.

The highly activated microglia correlate with learning deficit.

To explore the association between the changes in microglial phenotype with spatial learning and memory, we performed the Morris water maze on day 31 to 34 followed by microglia isolation in 24 mice included in the four experimental groups, normal, sham, mild TBI and severe TBI. The aim here was to investigate microglial phenotype within the hippocampus and thalamus as they are critical in the formation and processing of spatial learning and memory [21]. As expected, mice with severe TBI showed significant spatial learning and memory deficits (Figure 8, a). Furthermore, these mice showed increased highly activated microglia at 35 days post-injury (Figure 8, b). Using general linear regression, we found that the frequency of the highly activated microglia explained up to 47% of the variability observed in the cumulative latency to the platform, indicating a possible relationship between the existence of activated microglia and spatial learning/memory deficit chronically after the injury (Figure 8, c & d). Microglia clusters 1 and 2 did not contribute much to the model and showed no correlation with cumulative latency to platform.

Discussion

In the present study, we investigated whether CCI traumatic brain injury results in a spatiotemporal phenotypic change in microglia and if these changes are linked to a neurologic and cognitive deficit in a mouse model. Microglia are the brain immune cells, and they are implicated in almost all physiological processes in the CNS and play an important role in several inflammatory and neurodegenerative diseases. Chronic changes in microglia phenotype and function, support the notion that chronic microglial dysfunction may contribute to the chronic progressive neurodegeneration that are observed years after head injury [19]. However, the precise role of microglia in neuroinflammation following TBI and leading to neurological, sensory-motor and cognitive, deficits at acute, subacute, and chronic time points after TBI remain to be defined.

Here, we provided insights into the dynamics of several microglial marker expression after injury using multi-color flow cytometry coupled with an unbiased bioinformatics approach to characterize microglia in the different brain compartment after injury. We used CX3CR1 and the classical CD11b and CD45 [22] markers to identify microglia although we have also verified the cell lineage with microglia-specific marker TMEM119, and macrophage-specific marker CCR2 [23] (data not shown).

At 48 hrs after CCI, both the mild and severe TBI groups showed statistically significant sensory-motor and cognitive deficits compared to the sham animals [24]. At this acute time point, the number of microglia increased in the ipsilateral cortex in the mild injury group, while the number doubled in the severe TBI group in both hemispheres suggesting diffuse activation. Similar studies done in rodents described an increase from 2 to 20-fold of the number of cells in the injured brain [25,26]. An increase in the numbers of

isolated cells is attributed to resident microglia proliferation and expansion and peripheral cell infiltration [25,27]. It is reported that infiltrating monocytes and neutrophils respond quickly by crossing the blood-brain barrier and penetrating the injured tissue [27,28]. We found that infiltrating macrophages were only observed in the ipsilateral hemisphere of severe TBI (Figure 4) [29]. Surprisingly, infiltrating macrophages were not proinflammatory as they do not express TNFa and have a very high expression of CD206 the mannose receptor that is usually expressed on M2 macrophages, an observation in line with a previous report showing that macrophages in TBI have a mixed M1/M2 profile[30]. Interestingly, these cells were not found when the injury was mild, suggesting a possible threshold for the impact to solicit peripheral cells infiltration. Probably the mild injury produced here didn't result in the disruption of the blood-brain barrier which leads to limited recruitment of circulating myeloid cells to the injured site [31]. Although neutrophils have an important role post-injury as they are the first responders, we elected to focus on microglia as the cells most likely responsible for the long-term damage [32]. When we looked at microglia markers at 48 hours post-injury, we found that almost all markers were upregulated mainly on the ipsilateral side suggesting activation of these cells. Microglia activation corresponds to new biological functions [25]. These changes are readily visualized in immunohistochemistry imaging, previously reported in rodents [33–36]. Early activation of microglia after TBI has been observed in animal models [37–39] and in humans [40]. Persistent inflammation is also known to occur for up to one year after injury in rodents [41] and for several years in humans [42].

While there is agreement about the persistent activation of microglia after TBI, the phenotype and functional aspects of these microglia remain less clear. Earlier studies have focused on the increased number of microglia at different time point after injury [43] and morphological evidence of activation [44]. Using the M1/M2 phenotype scheme adapted from peripheral macrophages, researchers reported dysregulation of the anti-inflammatory M2 phenotype in association with chronic microglial activation [41,45,46]. However, mass cytometry and single-cell transcriptomic analysis reveal that microglia often present mixed phenotypes [47,48] and that the M1/M2 scheme may be an oversimplification[49].

An upregulation of Class II MHC and CD11b in chronically activated microglia [50] is consistent with our observations. High levels of CD11c and CD14 expression have been described in geriatric microglia, and chronic neuroinflammation may predispose to other neurologic disorders such as Alzheimer's disease [51].

In normal brains, our results showed that microglia are predominantly of cluster 1 with a ratio close to 2 to 1 in comparison to cluster 2, this was seen in all investigated regions. At 48 hours after injury, all the identified microglial populations increased in the injured brains as an indication of active proliferation. We noted at this time point a shift in the predominance between Cluster 1 and 2, suggesting that the injury microenvironment at 48 hours is pro-inflammatory as cluster 2 express significantly higher TNFa. As for cluster 3, these cells were found highly upregulated only in injured brain, even in mice that underwent the sham procedure.

At seven days post injury, the animals with mTBI showed complete recovery of motor deficits but not the sensory functions. Both sensory-motor functions remained impaired after the severe TBI. Both animal groups showed persistent spontaneous object recognition deficits post injury[52,53]. The highly activated microglia were nearly undetected at this time point with the persistence of the inflammatory cluster 2 in the cortex but not in the subcortical areas. Interestingly, at the chronic time point, sensory-motor and cognitive deficits were sustained post severe TBI and highly activated cells reappeared in injured brains along with persistence of cluster 2 cells suggesting an increase in the inflammatory background. An interesting observation in this study is the resolution of the highly activated microglia population at day 7 and its reappearance at the chronic time points. Previous studies have shown a bimodal change in microglia morphology [54] in the mouse model. This observation raises the possibility that after resolution of the acute injury, the second wave of activation may be triggered by late neuronal or axonal injury. This is in line with the delayed appearance of neurofibrillary tangles observed in humans after a single TBI [40].

In this study, we did not observe any patterns in the spatial distribution of the microglia populations in the severe TBI group suggesting that activation of microglia is already diffuse and includes ipsilateral, contralateral as well subcortical regions at 48 hours. In the mild TBI group, the proliferation of microglia was mostly observed on the ipsilateral cortex at 48hrs and ipsilateral cortex and hippocampus at 7 days.

Experimental studies in models of traumatic brain injury have shown that the majority of microglia and recruited macrophages at the site of injury have mixed pro and anti-inflammatory-like activation profiles, but that the anti-inflammatory-like response is short-lived and there is a phenotypic shift towards a proinflammatory-like dominant response within one week of injury [54]. Others have demonstrated prolonged activation of microglia in the subcortical areas at 28 days after injury [43,55]. Here, the identified macrophages profile fits an anti-inflammatory response at 48h. Whether macrophages and their cross-talk with microglia have a role in downregulating inflammation at 7 days is difficult to judge in our experimental setting [56]. Since both pro-and anti-inflammatory paths associated with overexpression of the same markers, it may be necessary to add additional parameters, such as cytokine expression [57]. In-depth characterization of the phenotype is also important for therapy after TBI as the timing of attenuating therapy delivery is critical for success [58].

Sensory-motor and cognitive deficits are prevalent post traumatic brain injury of all intensities and based on severity may persist for years after the injury[52,59] . Spontaneous object recognition and spatial learning and memory deficits found in this research are in line with our previous and other research studies[60,61]. Yet, to our knowledge few research characterized the cognitive deficits systematically over time, at acute, sub-acute and at chronic time points. The different tests used in this research study allowed for the early detection of the sensory motor and cognitive deficits and monitoring its persistence up to 35 days post injury while examining the course of microglial activation. The deficits seen after a TBI of mild intensity are often subtle and harder to detect in small animals. We have uncovered the sensory-motor and cognitive deficits at the acute and sub-acute time points in the animals with mild TBI. We have also found activation of the pro-inflammatory microglia at these same time points which warrant further

investigation and analysis of these early intervals, as it may shed light into a possible therapeutic window for TBI management of any intensity.

Finally, to link microglial phenotypes to cognitive deficit we have investigated the microglia response within the subcortical areas, as they are critical in the formation and processing of spatial learning, memory and relaying sensory and motor signals. The deficits seen on the MWM were increasing in relation to the severity of the injury as previously reported [62]. We found that each 1 % increase in the frequency of highly activated microglia at day 35 corresponds to an approximately 6-second increase in the cumulative latency to platform on the MWM indicating a decrease in the learning curve. Whether the presence of highly activated microglia is the cause of the spatial learning deficit cannot be concluded from our studies. The microglia may become activated by injured neurons or axons and requires further investigation. We also need to explore the same microglial activation pattern while using both cognitive tests, the spontaneous object recognition and the MWM at the acute phases in both mild and severe TBI.

Our study has some limitations; first, the panel of antibodies and the numbers of markers included are limited by the capacity of the conventional flow cytometer. Future studies using high throughput mass cytometry will be of interest. Second, sex differences are also reported comparing activation of microglia following TBI in adult female and male mice [63]; in our study, we used only male mice. In conclusion, using a nonbiased high-dimensional immune profiling of microglia in TBI, we revealed the immune landscape of sub-acute and chronic microglial activation. These results significantly extend our knowledge of how TBI affect long term deficits and will serve ultimately to define regions of interest and treatment windows to evaluate the efficacy of therapy.

Abbreviations

CCI: Controlled Cortical Impact

CNS: Central Nervous System

DPI: Days Post Injury

MFI : Mean Fluorescence Intensity

MWM: Maurice Water Maze

TBI: Traumatic Brain Injury

TSNE: t-distributed stochastic neighbor embedding

Declarations

Author contribution

Concept and design: SJK, HD, FK

Acquisition, analysis, and interpretation of data: ESS, MK, LN, HD, SJK

Drafting of the manuscript: ESS, HD, SJK

Statistical analysis: ESS, MK

Additional Information

This study was funded by the Office of Naval Research (ONR), ONRG - NICOP - N62909-17-1 2059 AWARD. The funders had no role in study design, data collection, analysis, decision to publish, or manuscript preparation.

All animals were treated in accordance with the International Guidelines for animal research. All procedures involving animals were approved by the Institutional Committee for the Care and Use of Laboratory Animals at the American University of Beirut

The authors declare that they have no known competing financial interests or personal relationships that could have appeared to influence the work reported in this paper.

Availability of data and materials

All data generated or analyzed during this study are included in this published article.

References

1. Wolf, S. A., Boddeke, H. W. G. M. & Kettenmann, H. Microglia in Physiology and Disease. *Annu. Rev. Physiol.* **79**, 619–643 (2017).
2. Yeh, H. & Ikezu, T. Transcriptional and Epigenetic Regulation of Microglia in Health and Disease. *Trends Mol. Med.* **25**, 96–111 (2019).
3. Nayak, D., Roth, T. L. & McGavern, D. B. Microglia development and function. *Annu. Rev. Immunol.* **32**, 367–402 (2014).
4. Tang, Y. & Le, W. Differential Roles of M1 and M2 Microglia in Neurodegenerative Diseases. *Mol. Neurobiol.* **53**, 1181–1194 (2016).
5. Hammond, T. R. *et al.* Single-Cell RNA Sequencing of Microglia throughout the Mouse Lifespan and in the Injured Brain Reveals Complex Cell-State Changes. *Immunity* **50**, 253–271.e6 (2019).
6. Nichols, M. R. *et al.* Inflammatory mechanisms in neurodegeneration. *J. Neurochem.* **149**, 562–581 (2019).
7. Perry, V. H., Nicoll, J. A. R. & Holmes, C. Microglia in neurodegenerative disease. *Nat. Rev. Neurol.* **6**, 193–201 (2010).

8. Hansen, D. V., Hanson, J. E. & Sheng, M. Microglia in Alzheimer's disease. *J. Cell Biol.* **217**, 459–472 (2018).
9. Geloso, M. C. *et al.* The Dual Role of Microglia in ALS: Mechanisms and Therapeutic Approaches. *Front. Aging Neurosci.* **9**, 242 (2017).
10. Ho, M. S. Microglia in Parkinson's Disease. *Adv. Exp. Med. Biol.* **1175**, 335–353 (2019).
11. Beschorner, R. *et al.* Differential regulation of the monocytic calcium-binding peptides macrophage-inhibiting factor related protein-8 (MRP8/S100A8) and allograft inflammatory factor-1 (AIF-1) following human traumatic brain injury. *Acta Neuropathol* **100**, 627–634 (2000).
12. Gentleman, S. M. *et al.* Long-term intracerebral inflammatory response after traumatic brain injury. *Forensic Sci. Int.* **146**, 97–104 (2004).
13. Whiteneck, G. G., Cuthbert, J. P., Corrigan, J. D. & Bogner, J. A. Prevalence of Self-Reported Lifetime History of Traumatic Brain Injury and Associated Disability: A Statewide Population-Based Survey. *J Head Trauma Rehabil* **31**, E55-62 (2016).
14. Skovira, J. W. *et al.* Cell cycle inhibition reduces inflammatory responses, neuronal loss, and cognitive deficits induced by hypobaria exposure following traumatic brain injury. *J. Neuroinflammation* **13**, 299 (2016).
15. Hernandez-Ontiveros, D. G. *et al.* Microglia activation as a biomarker for traumatic brain injury. *Front Neurol* **4**, 30 (2013).
16. Faden, A. I. Microglial activation and traumatic brain injury. *Ann. Neurol.* **70**, 345–346 (2011).
17. Redell, J. B. *et al.* Analysis of functional pathways altered after mild traumatic brain injury. *J. Neurotrauma* **30**, 752–764 (2013).
18. Meng, Q. *et al.* Traumatic Brain Injury Induces Genome-Wide Transcriptomic, Methylomic, and Network Perturbations in Brain and Blood Predicting Neurological Disorders. *EBioMedicine* **16**, 184–194 (2017).
19. Ritzel, R. M. *et al.* Sustained neuronal and microglial alterations are associated with diverse neurobehavioral dysfunction long after experimental brain injury. *Neurobiol. Dis.* **136**, 104713 (2020).
20. Wolf, Y. *et al.* Microglial MHC class II is dispensable for experimental autoimmune encephalomyelitis and cuprizone-induced demyelination. *Eur. J. Immunol.* **48**, 1308–1318 (2018).
21. Vorhees, C. V. & Williams, M. T. Assessing Spatial Learning and Memory in Rodents. *ILAR J.* **55**, 310–332 (2014).
22. Martin, E., El-Behi, M., Fontaine, B. & Delarasse, C. Analysis of Microglia and Monocyte-derived Macrophages from the Central Nervous System by Flow Cytometry. *J. Vis. Exp. JoVE* (2017) doi:10.3791/55781.
23. Li, Q., Lan, X., Han, X. & Wang, J. Expression of Tmem119/Sall1 and Ccr2/CD69 in FACS-Sorted Microglia- and Monocyte/Macrophage-Enriched Cell Populations After Intracerebral Hemorrhage. *Front. Cell. Neurosci.* **12**, (2019).

24. Fox, G. B., Fan, L., Levasseur, R. A. & Faden, A. I. Sustained Sensory/Motor and Cognitive Deficits With Neuronal Apoptosis Following Controlled Cortical Impact Brain Injury in the Mouse. *J. Neurotrauma* **15**, 599–614 (1998).
25. Susarla, B. T. S., Villapol, S., Yi, J.-H., Geller, H. M. & Symes, A. J. Temporal Patterns of Cortical Proliferation of Glial Cell Populations after Traumatic Brain Injury in Mice: http://dx.doi.org/10.1042/AN20130034 https://journals.sagepub.com/doi/10.1042/AN20130034 (2014) doi:10.1042/AN20130034.
26. Al Nimer, F. *et al.* Strain influences on inflammatory pathway activation, cell infiltration and complement cascade after traumatic brain injury in the rat. *Brain. Behav. Immun.* **27**, 109–122 (2013).
27. Toledano Furman, N. *et al.* High-resolution and differential analysis of rat microglial markers in traumatic brain injury: conventional flow cytometric and bioinformatics analysis. *Sci. Rep.* **10**, 11991 (2020).
28. McKee, C. A. & Lukens, J. R. Emerging Roles for the Immune System in Traumatic Brain Injury. *Front. Immunol.* **7**, (2016).
29. Morganti, J. M. *et al.* CCR2 Antagonism Alters Brain Macrophage Polarization and Ameliorates Cognitive Dysfunction Induced by Traumatic Brain Injury. *J. Neurosci.* **35**, 748–760 (2015).
30. Hsieh, C. L. *et al.* Traumatic brain injury induces macrophage subsets in the brain. *Eur. J. Immunol.* **43**, 2010–2022 (2013).
31. Alam, A. *et al.* Cellular infiltration in traumatic brain injury. *J. Neuroinflammation* **17**, 328 (2020).
32. Loane, D. J. & Kumar, A. Microglia in the TBI brain: The good, the bad, and the dysregulated. *Exp. Neurol.* **275**, 316–327 (2016).
33. Cao, T., Thomas, T. C., Ziebell, J. M., Pauly, J. R. & Lifshitz, J. Morphological and genetic activation of microglia after diffuse traumatic brain injury in the rat. *Neuroscience* **225**, 65–75 (2012).
34. Lier, J., Ondruschka, B., Bechmann, I. & Dreßler, J. Fast microglial activation after severe traumatic brain injuries. *Int. J. Legal Med.* **134**, 2187–2193 (2020).
35. Morrison, H., Young, K., Qureshi, M., Rowe, R. K. & Lifshitz, J. Quantitative microglia analyses reveal diverse morphologic responses in the rat cortex after diffuse brain injury. *Sci. Rep.* **7**, 13211 (2017).
36. Ritzel, R. M. *et al.* Functional differences between microglia and monocytes after ischemic stroke. *J. Neuroinflammation* **12**, 106 (2015).
37. Bye, N. *et al.* Transient neuroprotection by minocycline following traumatic brain injury is associated with attenuated microglial activation but no changes in cell apoptosis or neutrophil infiltration. *Exp. Neurol.* **204**, 220–233 (2007).
38. Chiu, C.-C. *et al.* Neuroinflammation in animal models of traumatic brain injury. *J. Neurosci. Methods* **272**, 38–49 (2016).
39. Elliott, M. B., Tuma, R. F., Amenta, P. S., Barbe, M. F. & Jallo, J. I. Acute Effects of a Selective Cannabinoid-2 Receptor Agonist on Neuroinflammation in a Model of Traumatic Brain Injury. *J.*

Neurotrauma **28**, 973–981 (2011).

40. Johnson, V. E. *et al.* Inflammation and white matter degeneration persist for years after a single traumatic brain injury. *Brain* **136**, 28–42 (2013).
41. Loane, D. J., Kumar, A., Stoica, B. A., Cabatbat, R. & Faden, A. I. Progressive Neurodegeneration After Experimental Brain Trauma: Association With Chronic Microglial Activation. *J. Neuropathol. Exp. Neurol.* **73**, 14–29 (2014).
42. Ramlackhansingh, A. F. *et al.* Inflammation after trauma: Microglial activation and traumatic brain injury. *Ann. Neurol.* **70**, 374–383 (2011).
43. Caplan, H. W. *et al.* Spatiotemporal Distribution of Microglia After Traumatic Brain Injury in Male Mice. *ASN NEURO* **12**, (2020).
44. d'Avila, J. C. *et al.* Microglial activation induced by brain trauma is suppressed by post-injury treatment with a PARP inhibitor. *J. Neuroinflammation* **9**, 31 (2012).
45. Kumar, A., Alvarez-Croda, D.-M., Stoica, B. A., Faden, A. I. & Loane, D. J. Microglial/Macrophage Polarization Dynamics following Traumatic Brain Injury. *J. Neurotrauma* **33**, 1732–1750 (2016).
46. Xu, H. *et al.* The Polarization States of Microglia in TBI: A New Paradigm for Pharmacological Intervention. *Neural Plasticity* vol. 2017 e5405104 https://www.hindawi.com/journals/np/2017/5405104/ (2017).
47. Mrdjen, D. *et al.* High-Dimensional Single-Cell Mapping of Central Nervous System Immune Cells Reveals Distinct Myeloid Subsets in Health, Aging, and Disease. *Immunity* **48**, 380–395.e6 (2018).
48. E. Hirbec, H., Noristani, H. N. & Perrin, F. E. Microglia Responses in Acute and Chronic Neurological Diseases: What Microglia-Specific Transcriptomic Studies Taught (and did Not Teach) Us. *Front. Aging Neurosci.* **9**, (2017).
49. Ransohoff, R. M. How neuroinflammation contributes to neurodegeneration. *Science* **353**, 777–783 (2016).
50. Izzy, S. *et al.* Time-Dependent Changes in Microglia Transcriptional Networks Following Traumatic Brain Injury. *Front. Cell. Neurosci.* **13**, (2019).
51. Graham, N. S. & Sharp, D. J. Understanding neurodegeneration after traumatic brain injury: from mechanisms to clinical trials in dementia. *J. Neurol. Neurosurg. Psychiatry* **90**, 1221–1233 (2019).
52. Fox, G. B., Fan, L., Levasseur, R. A. & Faden, A. I. Sustained Sensory/Motor and Cognitive Deficits With Neuronal Apoptosis Following Controlled Cortical Impact Brain Injury in the Mouse. *J. Neurotrauma* **15**, 599–614 (1998).
53. Yu, S. *et al.* Severity of controlled cortical impact traumatic brain injury in rats and mice dictates degree of behavioral deficits. *Brain Res.* **1287**, 157–163 (2009).
54. Jin, X., Ishii, H., Bai, Z., Itokazu, T. & Yamashita, T. Temporal Changes in Cell Marker Expression and Cellular Infiltration in a Controlled Cortical Impact Model in Adult Male C57BL/6 Mice. *PLOS ONE* **7**, e41892 (2012).

55. Thomas, T. C. *et al.* Does time heal all wounds? Experimental diffuse traumatic brain injury results in persisting histopathology in the thalamus. *Behav. Brain Res.* **340**, 137–146 (2018).
56. Hsieh, C. L. *et al.* Traumatic brain injury induces macrophage subsets in the brain. *Eur. J. Immunol.* **43**, 2010–2022 (2013).
57. Ziebell, J. M. & Morganti-Kossmann, M. C. Involvement of Pro- and Anti-Inflammatory Cytokines and Chemokines in the Pathophysiology of Traumatic Brain Injury. *Neurotherapeutics* **7**, 22–30 (2010).
58. Bedi, S. S. *et al.* Therapeutic time window of multipotent adult progenitor therapy after traumatic brain injury. *J. Neuroinflammation* **15**, (2018).
59. Fujimoto, S. T., Longhi, L., Saatman, K. E. & McIntosh, T. K. Motor and cognitive function evaluation following experimental traumatic brain injury. *Neurosci. Biobehav. Rev.* **28**, 365–378 (2004).
60. Darwish, H., Mahmood, A., Schallert, T., Chopp, M. & Therrien, B. Simvastatin and environmental enrichment effect on recognition and temporal order memory after mild-to-moderate traumatic brain injury. *Brain Inj.* **28**, 211–226 (2014).
61. Martínez-Drudis, L. *et al.* Delayed voluntary physical exercise restores “when” and “where” object recognition memory after traumatic brain injury. *Behav. Brain Res.* **400**, 113048 (2021).
62. Washington, P. M. *et al.* The Effect of Injury Severity on Behavior: A Phenotypic Study of Cognitive and Emotional Deficits after Mild, Moderate, and Severe Controlled Cortical Impact Injury in Mice. *J. Neurotrauma* **29**, 2283–2296 (2012).
63. Hanamsagar, R. *et al.* Generation of a microglial developmental index in mice and in humans reveals a sex difference in maturation and immune reactivity. *Glia* **65**, 1504–1520 (2017).
64. Sert, N. P. du *et al.* The ARRIVE guidelines 2.0: Updated guidelines for reporting animal research. *PLOS Biol.* **18**, e3000410 (2020).
65. Osier, N. D. & Dixon, C. E. The Controlled Cortical Impact Model: Applications, Considerations for Researchers, and Future Directions. *Front. Neurol.* **7**, (2016).
66. Matsuura, K., Kabuto, H., Makino, H. & Ogawa, N. Pole test is a useful method for evaluating the mouse movement disorder caused by striatal dopamine depletion. *J. Neurosci. Methods* **73**, 45–48 (1997).
67. Hebda-Bauer, E. K. *et al.* Forebrain glucocorticoid receptor overexpression increases environmental reactivity and produces a stress-induced spatial discrimination deficit. *Neuroscience* **169**, 645–653 (2010).
68. Vorhees, C. V. & Williams, M. T. Morris water maze: procedures for assessing spatial and related forms of learning and memory. *Nat. Protoc.* **1**, 848–858 (2006).
69. Spijker, S. Dissection of Rodent Brain Regions. in *Neuroproteomics* (ed. Li, K. W.) 13–26 (Humana Press, 2011). doi:10.1007/978-1-61779-111-6_2.
70. Lee, J.-K. & Tansey, M. G. Microglia isolation from adult mouse brain. *Methods Mol. Biol. Clifton NJ* **1041**, 17–23 (2013).

71. Parks, D. R., Roederer, M. & Moore, W. A. A new ‘Logicle’ display method avoids deceptive effects of logarithmic scaling for low signals and compensated data. *Cytom. Part J. Int. Soc. Anal. Cytol.* **69**, 541–551 (2006).
72. Maaten, L. van der & Hinton, G. Visualizing Data using t-SNE. *J. Mach. Learn. Res.* **9**, 2579–2605 (2008).
73. Grün, D. *et al.* Single-cell messenger RNA sequencing reveals rare intestinal cell types. *Nature* **525**, 251–255 (2015).

Figures

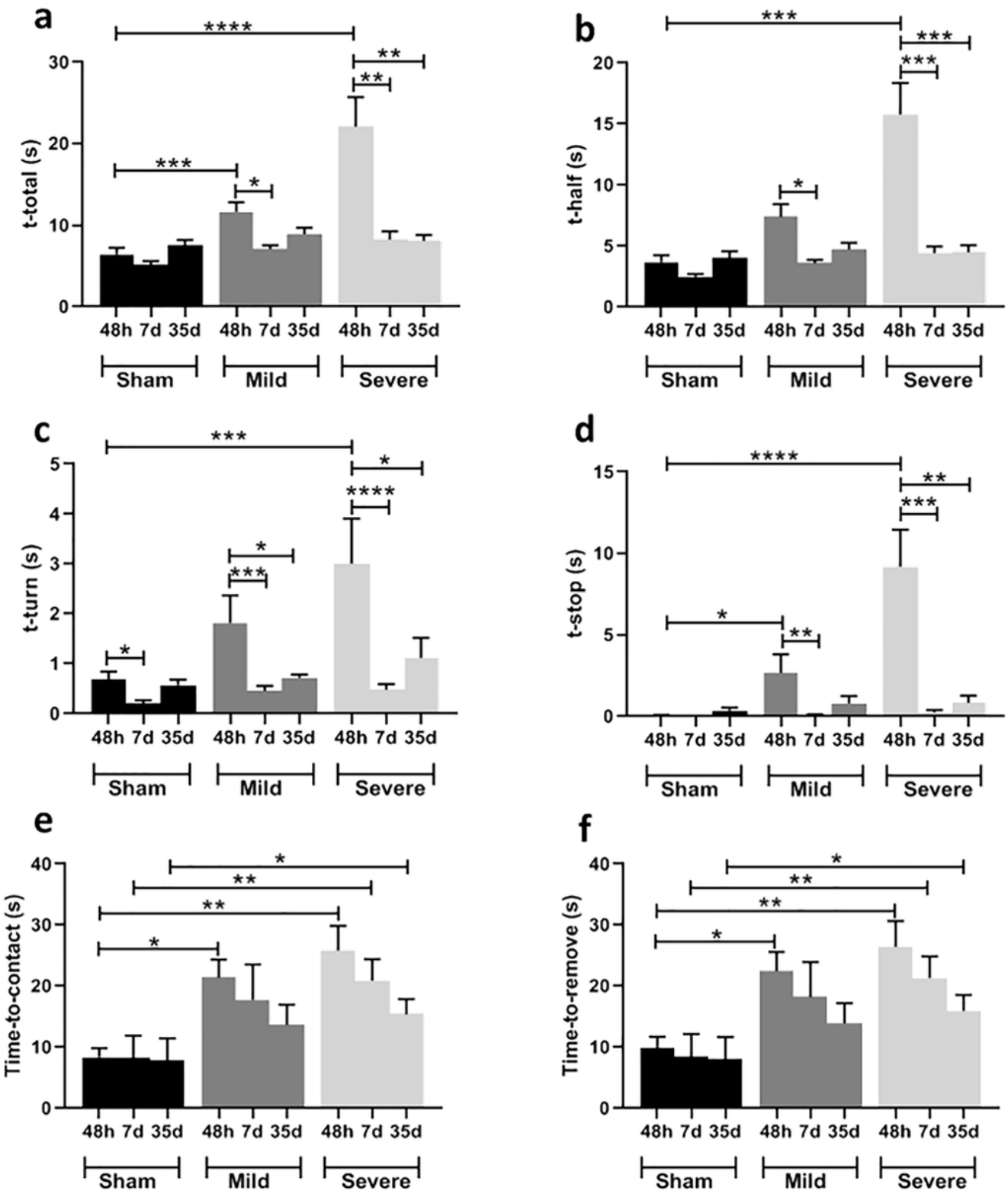

Figure 1

Neurological tests: (a-d) Pole climbing test. (a) t-total: Time needed to reach the bottom of the vertical rough-surfaced pole. (b) t-half: time needed to reach half of the pole. (c) t-turn: time at which the mouse turned head down on the pole. (d) t-stop: Amount of time mouse stopped on the pole. (e-f) Adhesive removal test. (e) The time needed to sense (time-to-contact) and (f) to remove (time-to-remove) the tape.

Kruskal-Wallis test followed by Dunnett's multiple comparison post-test. *p < 0.05, **p < 0.01, ***p < 0.001, ****p < 0.0001

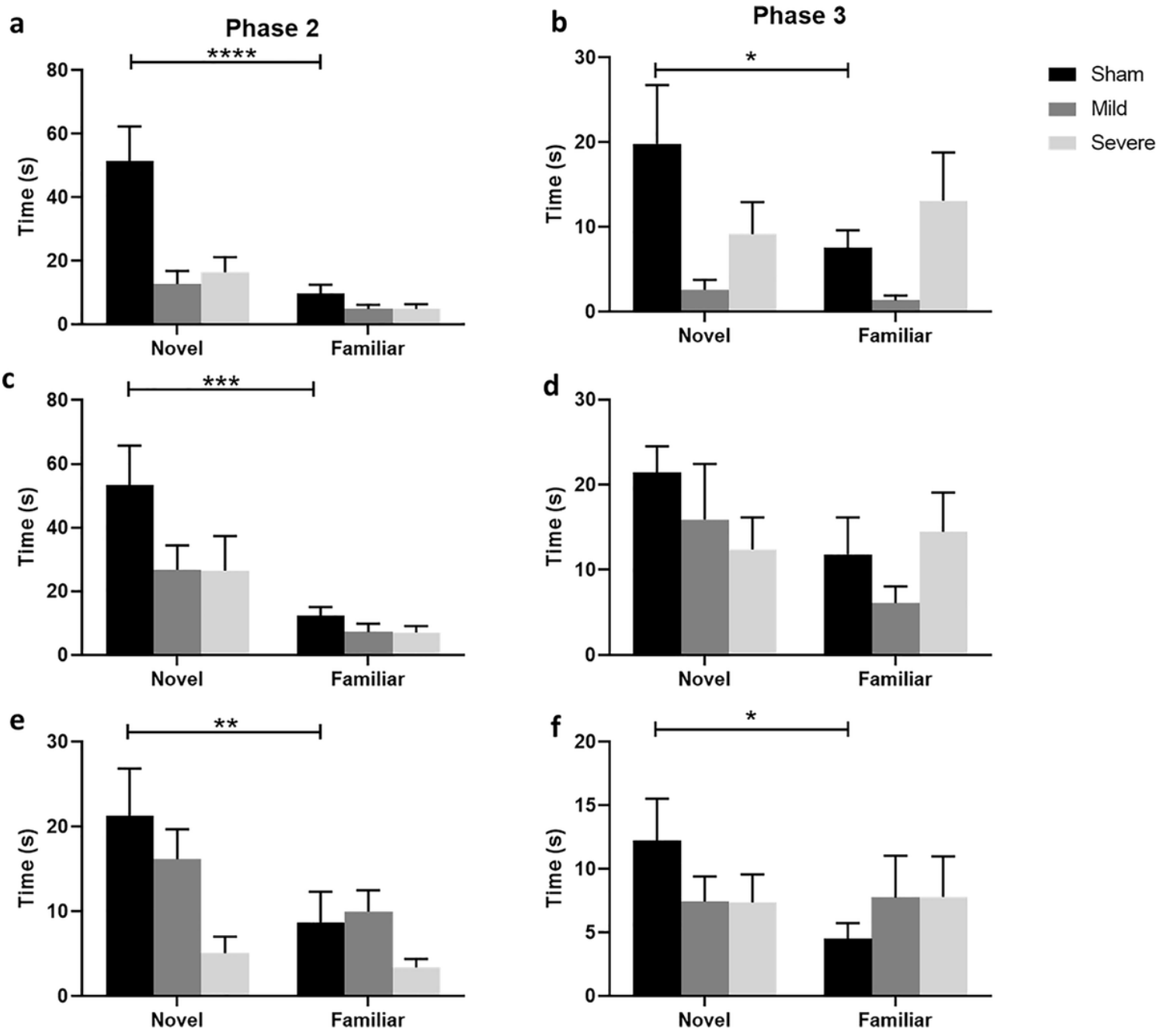

Figure 2

Time spent exploring the novel versus familiar objects during phase 2 (novel object) and phase 3 (novel location) of spontaneous object and location recognition memory test at 48h (A-B), 7 days (C-D) and 35 days (S-F). Kruskal-Wallis test followed by Dunnett's multiple comparison post-test. *p < 0.05, **p < 0.01, ***p < 0.001, ****p < 0.0001.

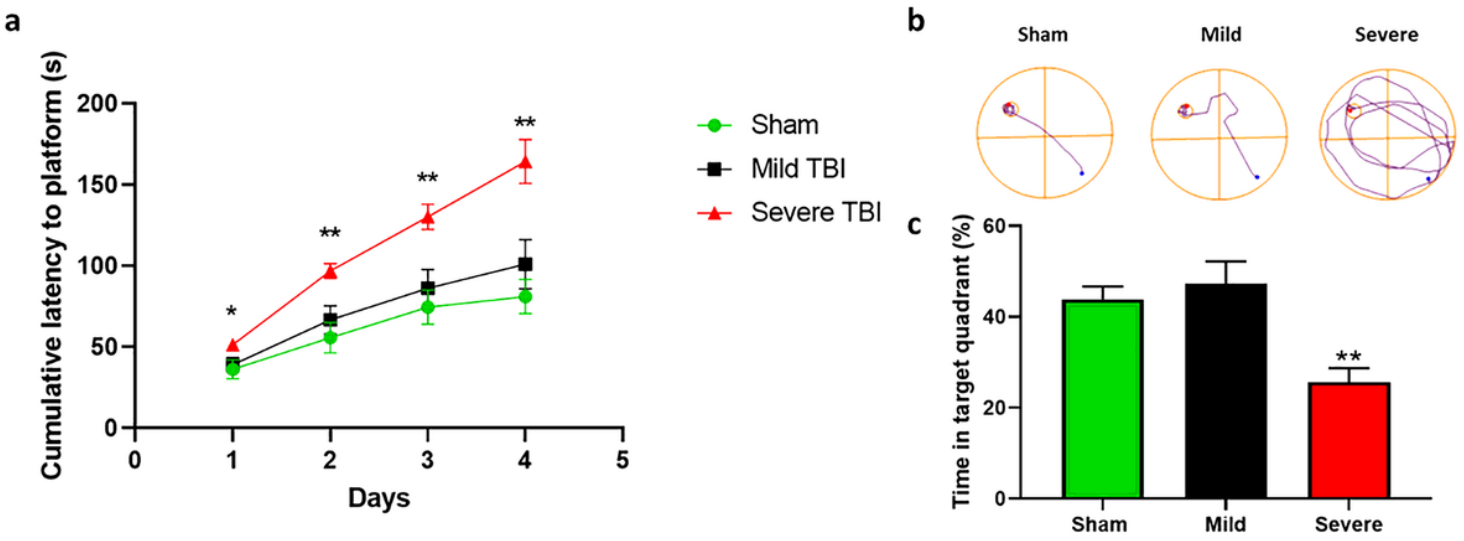

Figure 3

Morris water maze at 35 days (a) Escape latency to reach the platform between different groups presented as a cumulative time to the platform. (b) Representative Morris water maze performance in different groups, n = 10/group. (c) In the MWM probe trial, time spent in the target quadrant. Kruskal-Wallis test followed by Dunnett's multiple comparison post-test. *p < 0.05, **p < 0.01, ***p < 0.001, ****p < 0.0001.

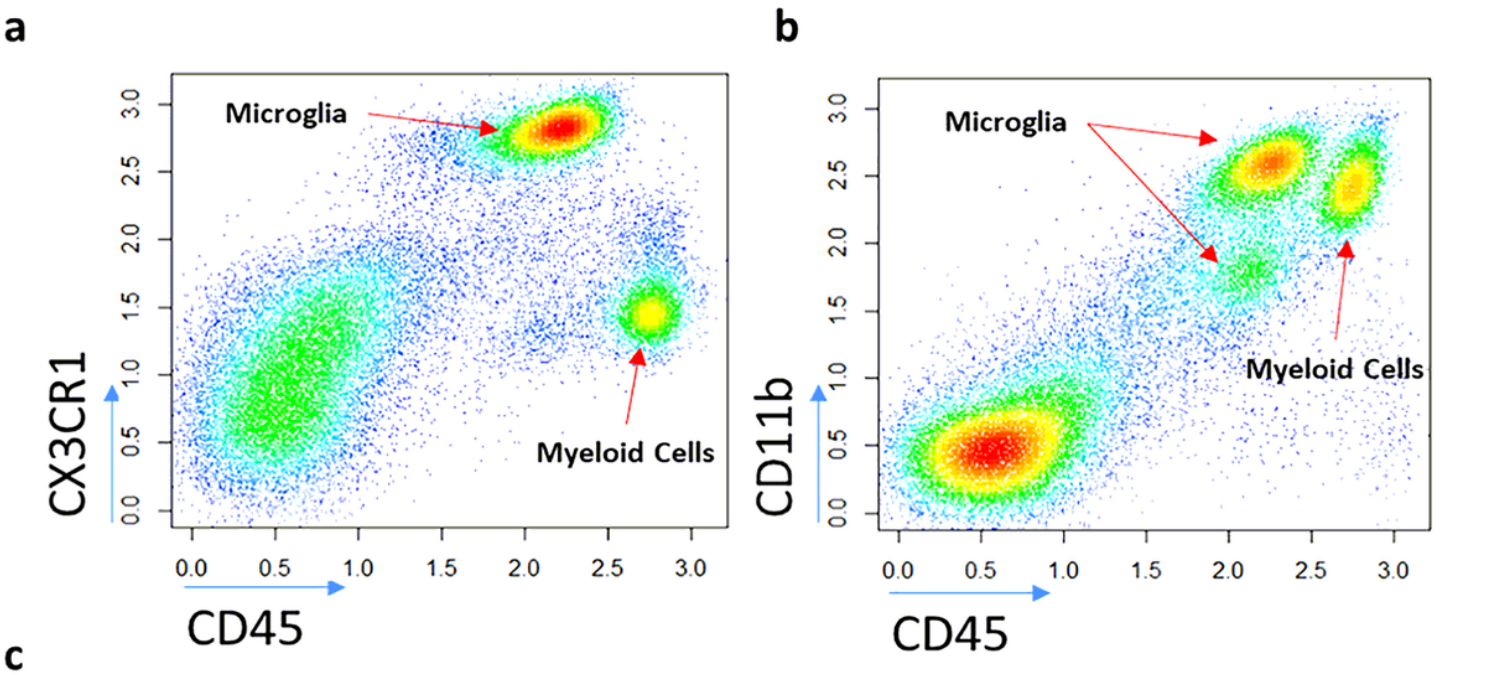

c

Time	Regions	Sides	Microglia				Myeloid Cells			
			Normal	Sham	Mild TBI	Severe TBI	Normal	Sham	Mild TBI	Severe TBI
48 Hours	*Hyppocampus*	Contralateral	0.48%	0.47%	0.28%	**1.20%**	0.00%	0.00%	0.01%	0.03%
		Ipsilateral	0.49%	0.48%	0.30%	**1.28%**	0.01%	0.01%	0.00%	**1.89%**
	Thalamus	Contralateral	0.99%	1.01%	0.97%	**1.83%**	0.00%	0.00%	0.01%	0.03%
		Ipsilateral	0.99%	0.96%	1.11%	**1.72%**	0.00%	0.01%	0.01%	**1.34%**
	Cortex	Contralateral	1.71%	2.17%	2.17%	**3.94%**	0.01%	0.06%	0.02%	0.04%
		Ipsilateral	1.62%	2.00%	**2.84%**	**4.35%**	0.01%	0.05%	0.16%	**1.85%**
7 Days	*Hyppocampus*	Contralateral	0.45%	0.50%	0.48%	**0.64%**	0.00%	0.00%	0.01%	0.00%
		Ipsilateral	0.43%	0.43%	0.40%	**0.69%**	0.00%	0.00%	0.02%	0.00%
	Thalamus	Contralateral	1.00%	1.16%	1.09%	1.22%	0.00%	0.00%	0.01%	0.00%
		Ipsilateral	0.92%	0.80%	0.86%	**1.53%**	0.00%	0.01%	0.00%	0.01%
	Cortex	Contralateral	1.62%	2.21%	**2.60%**	**2.44%**	0.01%	0.00%	0.00%	0.06%
		Ipsilateral	1.70%	1.92%	**2.35%**	**2.49%**	0.00%	0.00%	0.01%	0.02%
35 Days	*Hyppocampus*	Contralateral	0.46%	0.43%	0.47%	**0.71%**	0.00%	0.01%	0.02%	0.00%
		Ipsilateral	0.47%	0.33%	0.68%	**0.88%**	0.02%	0.00%	0.00%	0.02%
	Thalamus	Contralateral	0.95%	0.89%	1.02%	**1.43%**	0.00%	0.01%	0.01%	0.00%
		Ipsilateral	0.90%	0.90%	1.11%	1.18%	0.00%	0.01%	0.00%	0.02%
	Cortex	Contralateral	2.03%	1.84%	1.81%	**2.35%**	0.00%	0.00%	0.01%	0.01%
		Ipsilateral	1.80%	2.04%	2.14%	2.15%	0.00%	0.01%	0.00%	0.00%

Figure 4

Flow cytometry staining of microglia and other myeloid cells. (a) Representative scatter plot using microglial marker CD45 and CX3CR1. (b) Representative scatter plot using microglial marker CD45 and CD11b. (c) Percentage of cells for each of the experimental group at the various time points in the 3 brain regions. Bold numbers in red are considered significant ($p < 0.05$) by fisher exact test in comparison to the sham group of the same time point.

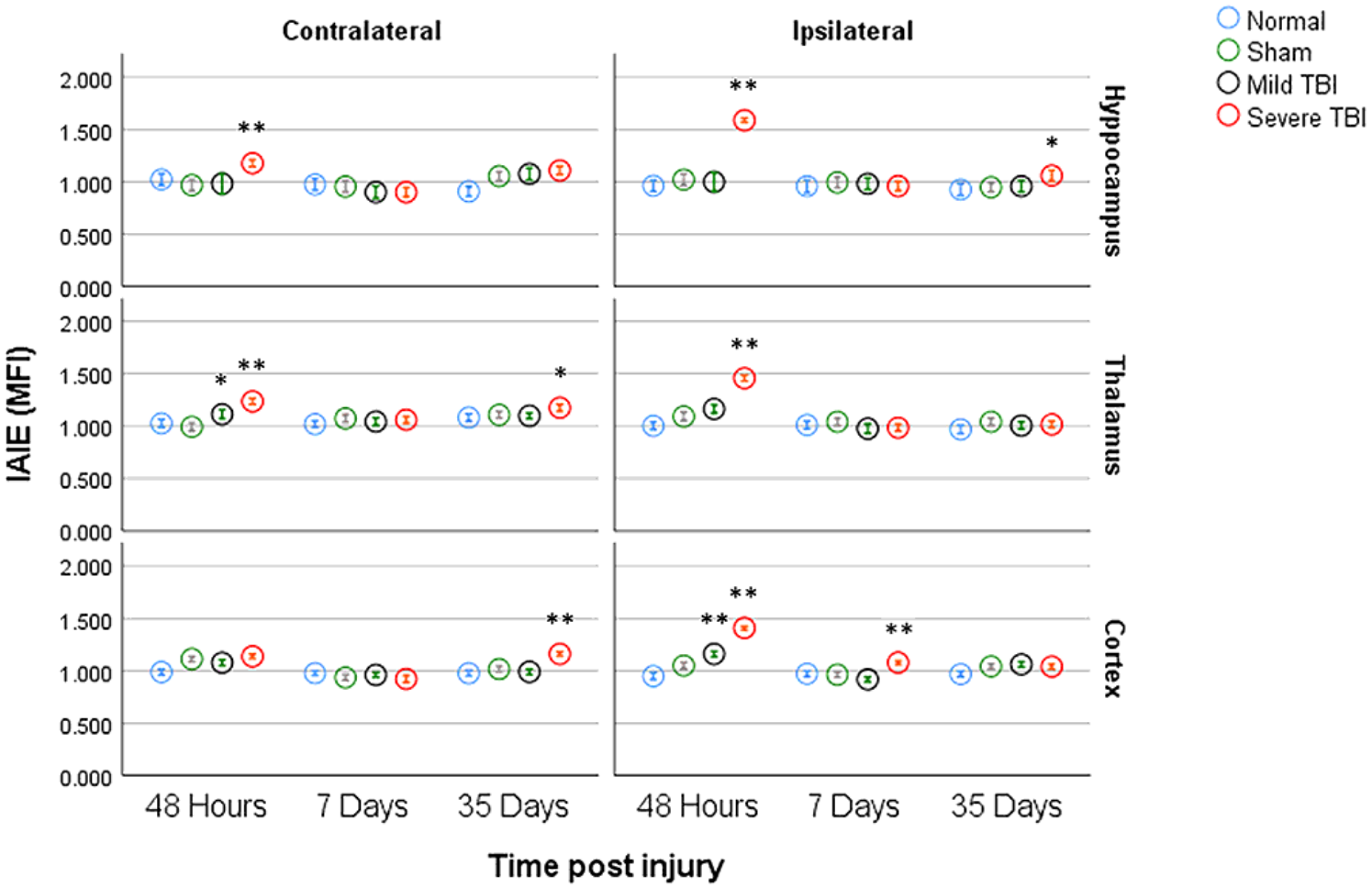

Figure 5

Microglial IAIE mean fluorescence intensity detected by FACS presented per group, time points, regions, and sides. Significance is calculated in reference to the sham of the same condition using ANOVA followed by Bonferroni correction for multiple comparisons *p < 0.05, **p < 0.01.

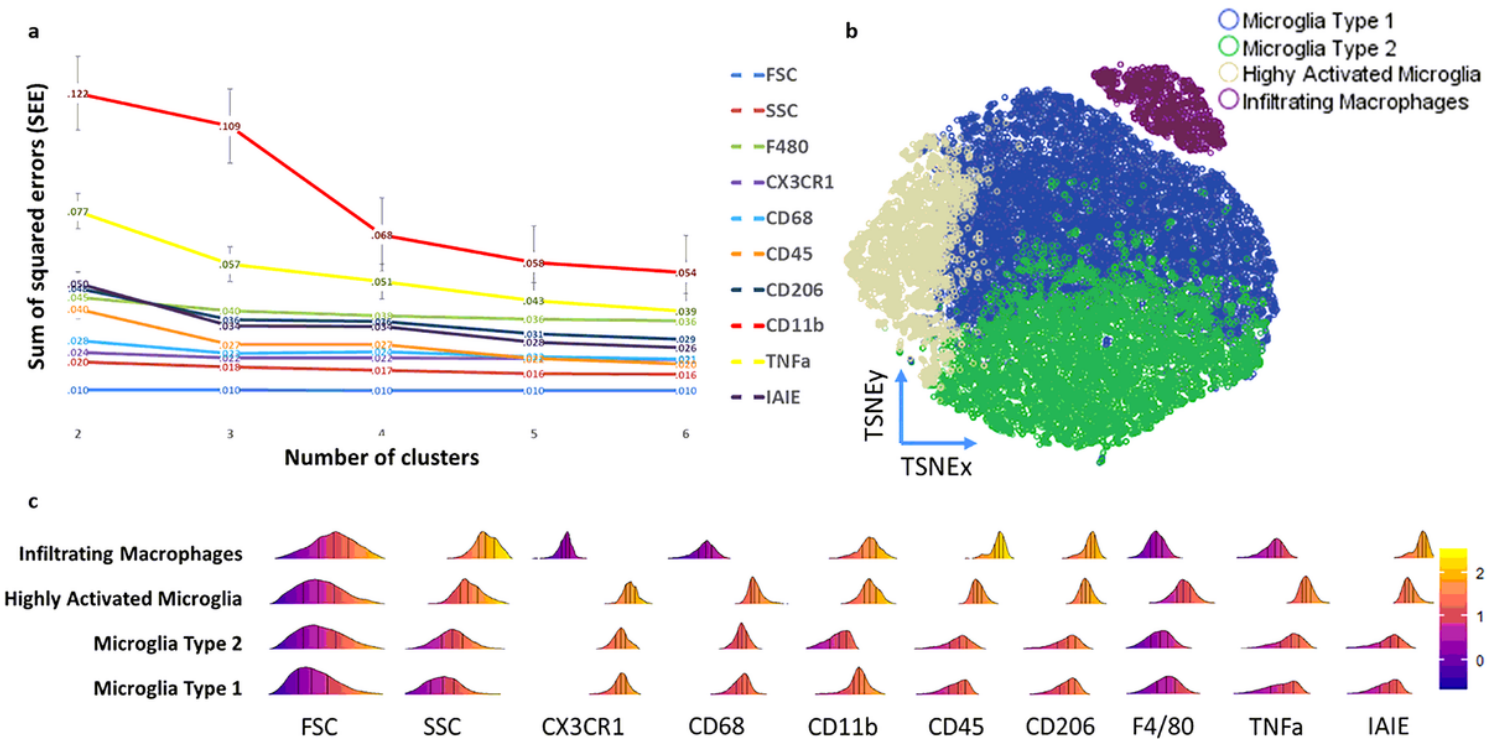

Figure 6

Non-linear dimensionality reduction using t-distributed stochastic neighbor embedding (t-SNE) and cluster analysis. (a) Sum of the squared error to identify the markers with the highest variability among clusters. (b) TSNE plot showing the four different clusters. (c) The distributions of the different markers in relation to the four identified clusters.

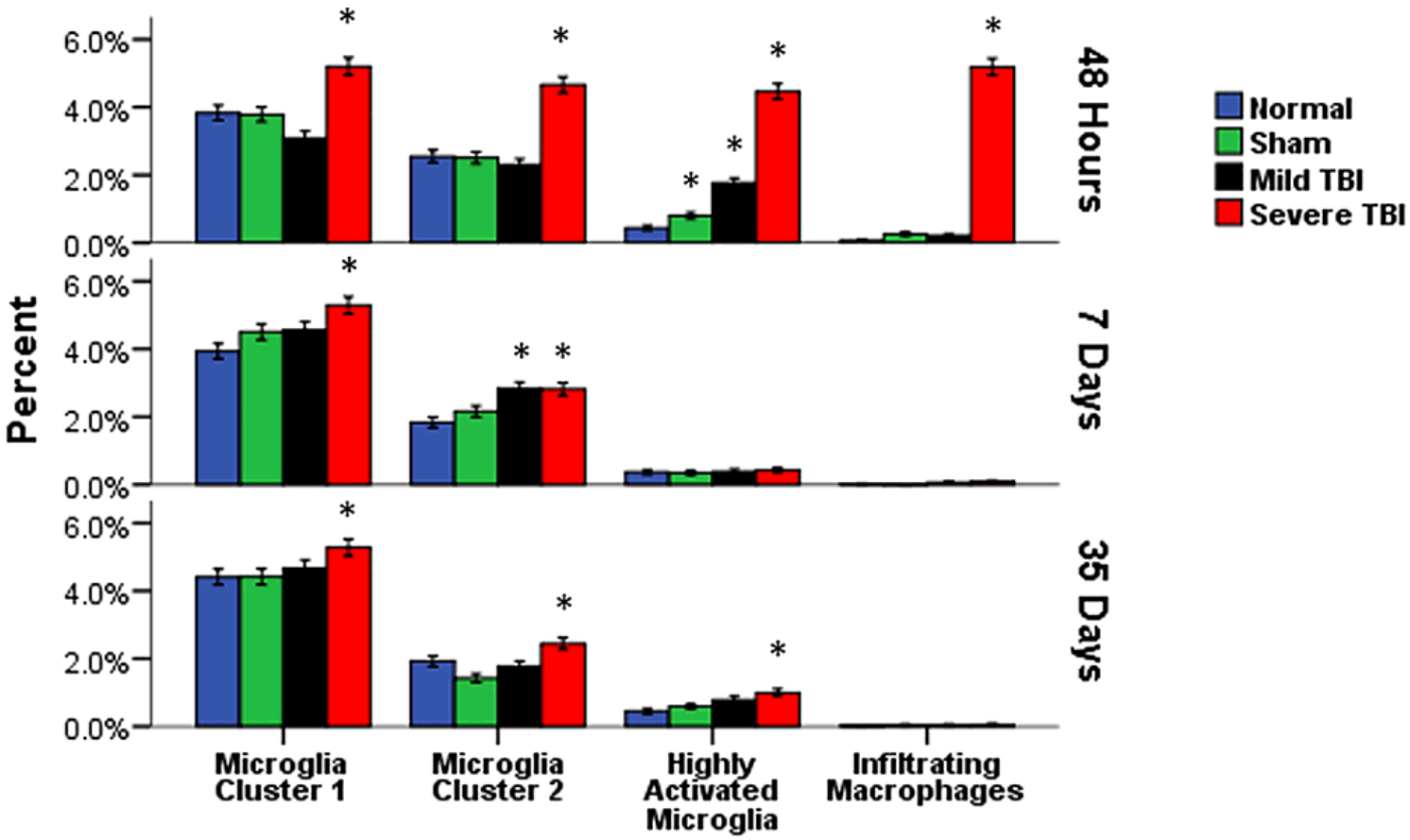

Figure 7

Overall Percentage of cell clusters per group, time points, and regions. Significance is calculated in reference to the Sham by Chi-square test followed by Bonferroni for multiple comparison post-test. *p < 0.05.

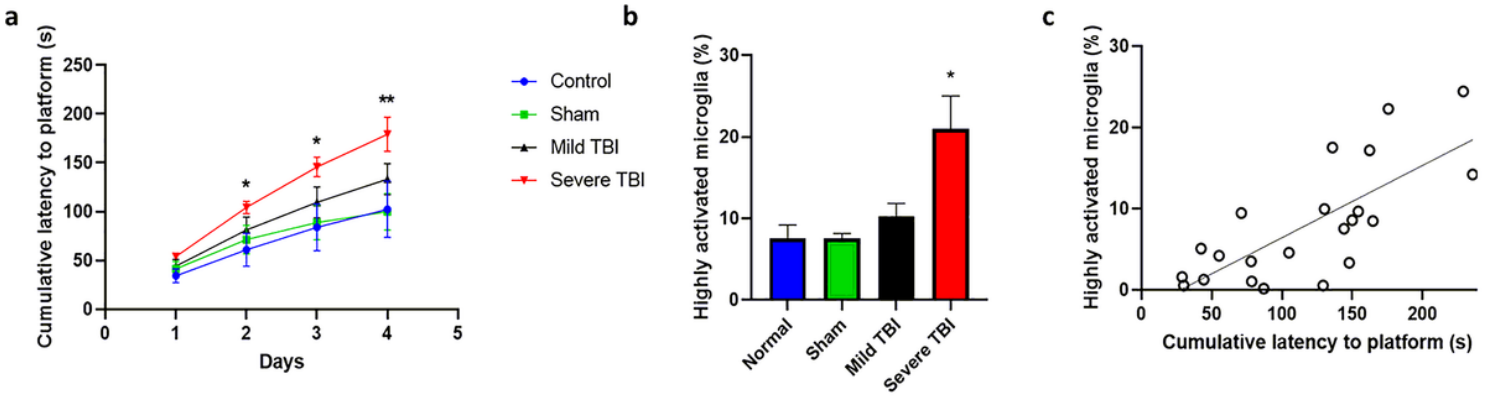

d

Model	Unstandardized Coefficients		Standardized Coefficients			95.0% Confidence Interval for B		Correlations		
	B	Std. Error	Beta	t	Sig.	Lower Bound	Upper Bound	Zero-order	Partial	Part
(Constant)	68.408	20.734		3.299	0.004	24.846	111.969			
Microglia Cluster 1	-0.092	0.609	-0.040	-0.150	0.882	-1.371	1.188	-0.104	-0.035	-0.024
Microglia Cluster 2	0.215	1.310	0.044	0.164	0.871	-2.538	2.969	0.130	0.039	0.026
Highly activated microglia	6.087	1.453	0.730	4.188	0.001	3.034	9.140	0.742	0.703	0.661

a. Dependent Variable: Cumulative latency to platform (s)

Figure 8

The relation between spatial learning deficit and microglia activation. (a) Cumulative latency to platform showing spatial learning curve and deficit in severe TBI group. (b) Frequency of highly activated microglia in subcortical areas. (c) Pearson correlation between cumulative latency to the platform and activated microglia frequency. (d) Linear regression output showing the relationship between the different cell clusters and the cumulative latency to the platform (dependent variable). (*p < 0.05).

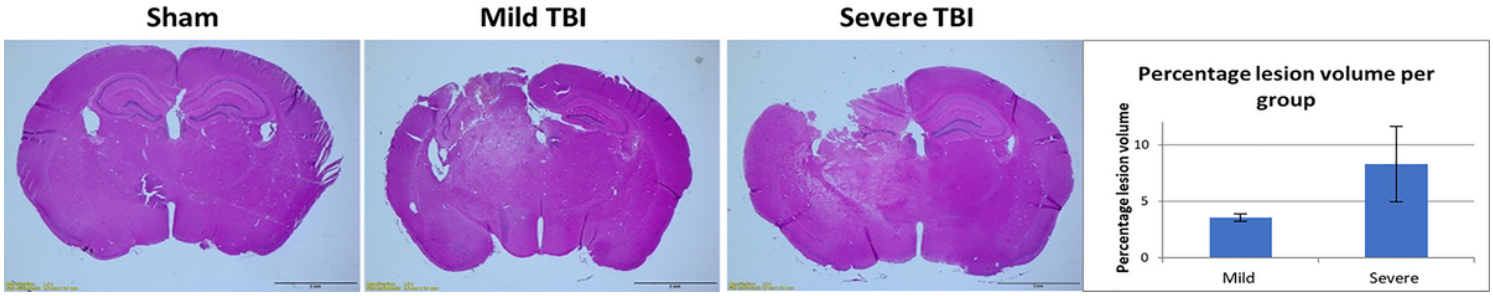

Figure 9

Controlled cortical impact (CCI)-induced brain injury. Representative sections shown were stained with hematoxylin and eosin. The data represent the percentage lesion volume as assessed two days following the impact. The mean lesion volume of the animals with severe injury (n = 3; 8.31% ± 3.35) was more significant than the animals with mild injury (n = 2; 3.58% ± 0.33).